UC Davis

UC Davis Previously Published Works

Title

Nanomechanical Characterization of Micellar Surfactant Films via Atomic Force Microscopy at a Graphite Surface

Permalink

https://escholarship.org/uc/item/7gb7n4fv

Journal

Langmuir, 33(9)

ISSN

0743-7463

Authors

Micklavzina, Benjamin L
Zhang, Shengwei
He, Hao
et al.

Publication Date

2017-03-07

DOI

10.1021/acs.langmuir.6b04315

Peer reviewed

eScholarship.org Powered by the California Digital Library
University of California

This document is confidential and is proprietary to the American Chemical Society and its authors. Do not copy or disclose without written permission. If you have received this item in error, notify the sender and delete all copies.

Nanomechanical Characterization of Micellar Surfactant Films Via Atomic Force Microscopy at a Graphite Surface

Journal:	*Langmuir*
Manuscript ID	la-2016-043154.R2
Manuscript Type:	Article
Date Submitted by the Author:	04-Feb-2017
Complete List of Authors:	Micklavzina, Benjamin; University of California Davis, Materials Science and Engineering Zhang, Shengwei; Zhejiang University, Department of Polymer Science and Engineering He, Hao; Zhejiang University, Department of Materials Science and Engineering Longo, Marjorie; University of California Davis, Department of Chemical Engineering

SCHOLARONE™
Manuscripts

Nanomechanical Characterization of Micellar Surfactant Films Via Atomic Force Microscopy at a Graphite Surface

*Benjamin L. Micklavzina,[†] Shengwei Zhang,[‡] Hao He,[¶] and Marjorie L. Longo[§,]**

[†]Department of Materials Science and Engineering, University of California Davis, Davis, California, 95616,

[‡]Department of Polymer Science and Engineering, Zhejiang University, Hangzhou 310027, China

[¶] Department of Materials Science and Engineering, Zhejiang University, Hangzhou 310027, China

[§]Department of Chemical Engineering, University of California Davis, Davis, California, 95616

ABSTRACT

In this work, we study the mechanical properties of sodium dodecylsulfate (SDS) and dodecylamine hydrochloride (DAH) micellar films at a graphite surface via atomic force microscopy (AFM). Breakthrough forces for these films were measured using silicon nitride cantilevers, and found to be 1.1 $\pm$0.1 nN for a 10 mM DAH film and 3.0 $\pm$0.3 nN for a 10 mM SDS film. For 10 mM SDS films, it was found that the addition of 1.5 mM of NaCl, Na_2SO_4, or $MgCl_2$ produced a 50-70% increase in measured breakthrough force. Similar results were found for 10 mM DAH films when NaCl and $MgCl_2$ were added. A model was developed, based upon previous work on lipid films and CMC data gathered via spectrofluorometry measurements, to

predict the change in normalized breakthrough forces with added salt concentrations for SDS and DAH films. Using this model, it was found that the activation volume required to initiate breakthrough was roughly 0.4 nm^3 for SDS and 0.3 nm^3 for DAH, roughly the volume of a single molecule. Normalized breakthrough force data for SDS films with added $MgCl_2$ showed an unexpected dip at low added salt concentrations. The model was adapted to account for changing activation volumes, and a curve of activation volume versus magnesium concentration was obtained, showing a minimum volume of 0.21 nm^3. The addition of 0.2 mM SDS to a 10 mM DAH solution was found to double the measured breakthrough force of the film. Images taken of the surface showed a phase change from cylindrical hemimicelles to a planar film that may have produced the observed differences. The pH of the bulk solution was varied for both 10 mM SDS and DAH films, and was found to have little effect on breakthrough force.

INTRODUCTION

A great deal of work has been done studying the nanostructures formed by surfactants at hydrophobic surfaces. Atomic force microscopy (AFM) is a particularly useful tool for examining these structures, as it allows direct imaging of micellar surface structures. Manne et al. first imaged these structures for sodium dodecylsulfate (SDS).[1] They found that, when exposed to a highly ordered pyrolytic graphite (HOPG) surface, SDS spontaneously formed hemicylindrical wormlike micelles at the graphite interface. These micelles, typically several nanometers in width, were found to arrange in large micrometer sized grains along the surface. Additional AFM studies of surfactants at graphite surfaces have been performed for other surfactants as well as some surfactant/surfactant and surfactant/salt mixtures.[2-6] However, while the geometry of these surface structures is well documented, their mechanical properties are less studied. Early work suggests that these thin surfactant films are fragile, and that the delicate

surface structures can be damaged or destroyed at high imaging forces.[7-8] Work done with mixtures of cationic and anionic surfactants also indicates a strengthening of the surface upon mixing, as well as the potential for phase changes from hemicylindrical micelles to hemispheres or flat monolayers.[9-10]

AFM has also been a common tool in the study of supported lipid layers, which share many physical similarities to supported surfactant assemblies.[11-12] In the studies of lipid layers using this method, one of the most commonly applied methods for mechanical characterization has been measuring the force required for the AFM tip to break through the film to the surface beneath, usually called the breakthrough force.[13-15] Breakthrough forces for supported lipid layers are well studied, and a number of well accepted models exist which can be used to explain and quantify breakthrough events.[13, 16-17] It is generally thought that breakthrough events begin with the creation of a void beneath the tip. Once this void reaches a critical size, the activation volume, the tip rapidly reaches the surface. This activation volume is accompanied by an activation energy, which is the energy required to create the void. The activation energy is dependent upon the energetically unfavorable head-head repulsion and the energetically favorable hydrophobic tail-tail interactions. Several other factors are known to influence breakthrough forces measured in supported lipid films. It has been shown that zwitterionic lipid films strengthen in the presence of salts due to a phenomenon known as salt-bridging, where counterions align between head group charges and increase packing density at the surface.[12, 18] It is also generally accepted that lipids with longer hydrocarbon tails are stiffer, and that their films are harder to puncture.[19] While we expect that zwitterionic lipid and single tailed surfactant films will share similar trends, there are also enough fundamental differences (surface charge density,

liquid ordered/disordered phases, packing parameter, tip/surface geometries) between them that it cannot be assumed they will behave identically.

Here, we examine the mechanical properties of surfactant films using the well-established method that has been used for supported lipid systems, namely by examining the breakthrough force of the micellar film. We also explore the effects on the breakthrough force of adding salts and cosurfactants into solution, with the overall goal of developing a model relationship between added concentration and surface strength. Our work will demonstrate that the strengthening mechanism of these films in the presence of salts is distinct from that seen in lipids, and that the overall strength of the film is strongly correlated with both the free energy of micellization and the ionic species bound to the surface.

MATERIALS AND METHODS

Surfactant Film Formation. Sodium dodecylsulfate (SDS) was purchased from Sigma-Aldrich (ACS reagent, ≥99%) and used to prepare 15 mL solutions of 5-25 mM SDS in deionized water. Dodecylammonium chloride (DAH) was purchased from TCI America (≥98%) and used to prepare 15 mL solutions of 7.5-25 mM solutions in deionized water. Each solution was allowed to equilibrate with ZYH grade highly ordered pyrolytic graphite (HOPG) purchased from MikroMasch for thirty minutes to one hour. Before each trial, the graphite surface was cleaved with Scotch tape to ensure that a clean surface was available for adsorption.

AFM Imaging and Image Analysis. Equilibrated surfaces at 25°C were then examined using a Dimension 3100 AFM with a Nanoscope IVa controller and MSCT non-conductive silicon nitride tips from Veeco using cantilevers with spring constants of 0.05 Nm^{-1}. Images were taken in tapping mode using scan rates between 0.5-2.5 Hz and integral and proportional gains fixed at 2:3 ratios respectively. Imaging was done in the repulsive force regime, not in direct contact with

the surface. As such, height information was not obtained. Images shown represent vertical deflection of the cantilever due to repulsive forces. The presence of surface features was verified by modifying scan angle and observing the change in angle of the recorded image. All dimensional measurements of surface features use standard error $\left(\frac{SD}{\sqrt{N}}\right)$,where SD is the standard deviation and N is the number of measurements, to account for uncertainty.

Breakthrough Force Measurements. Equilibrated surfaces at 25°C were probed using 0.05 Nm^{-1} MSCT non-conductive silicon nitride tips from Veeco, and the breakthrough forces were measured and recorded using the same tip at the same surface location. Ramp rates when taking force curves were kept constant throughout each trial at 50 nms^{-1}. Once sufficient numbers of breakthrough events were obtained (n∼50 necessary to perform a Gaussian fit), the tip was lifted from the surface by 10 nm before adding stock solutions of salts to the water. The salts used were magnesium chloride hexahydrate from Sigma-Aldrich (ACS reagent, ≥99%), sodium sulfate from Sigma-Aldrich (ACS reagent, ≥99%), and sodium chloride from Fischer Scientific (ACS reagent, ≥99%). SDS and DAH were added to the solution as necessary to preserve the 10 mM surfactant concentration during experiments. After the addition of salt to the solution, the system was given forty minutes to equilibrate before returning the tip to the surface for measurement. This equilibration time was determined to be adequate by looking at the change in surface properties with time (see Supporting Information). Using this approach, we measured the breakthrough force of the same surface area using the same AFM tip at varying salt concentrations. The magnitude of breakthrough events was recorded as the force above which contact with the graphite was reached. Breakthrough forces were measured manually for each recorded force curve.

Experiments were also done measuring the effect of pH change on breakthrough forces. The procedure for these measurements was identical to that of the salts described above, though the pH changes were not measured directly. Solutions of dilute hydrochloric acid from Fischer Scientific (ACS reagent plus) were used to alter the pH of 10 mM SDS solutions during experiments, and pH was measured in a separate container with the same concentrations of SDS and HCl as in the sample container. The pH of the 10 mM DAH solution was altered using dilute sodium hydroxide from Fischer Scientific (ACS reagent, ≥99%), and the pH of the sample was measured indirectly using the same method as with SDS. All pH measurements were made with a Checker pH Meter from Hanna Instruments.

Critical Micelle Concentrations. Solutions of SDS or DAH were prepared with fixed salt concentrations. These solutions (3 mL) were placed in 3.5 mL UV Fluorometer methacrylate cuvettes from Perfector Scientific. Then, 44μL of a 10 mM solution of 1,6 diphenyl 1, 3, 5 hexatriene (DPH) from Sigma-Aldrich was added to this solution and gently stirred at 25°C. Fluorescence anisotropy measurements were taken using a Jasco FP-8500 Spetrofluorometer, and the measured r-factor was used to determine the critical micelle concentration (see Supporting Information).

RESULTS AND DISCUSSION

AFM Imaging of SDS Films. Our first goal was to recreate previous studies on the adsorbed structure of sodium dodecylsulfate (SDS) films at graphite surfaces as a way to establish a baseline for our work. AFM imaging has shown that SDS at concentrations above 5 mM, well below the established CMC of 7.8 mM, will form long rows of hemicylindrical micelles when exposed to bare graphite.[2, 5] Displayed in Figure 1 are our images taken of SDS films at varying concentration. The micellar spacing varies with respect to the SDS concentration, decreasing

from a periodicity of 6.7±0.1 nm at 7.5 mM to 4.5±0.1 nm at 15 mM. Increasing the SDS concentration further did not yield significant changes in the intermicellar width. These values are in good agreement with previous work, and imply that the scale of our images is correctly calibrated.[2, 5] Addition of 20 mM NaCl showed a slight increase in the micellar periodicity from 4.5±0.1 nm to 4.8±0.1 nm.

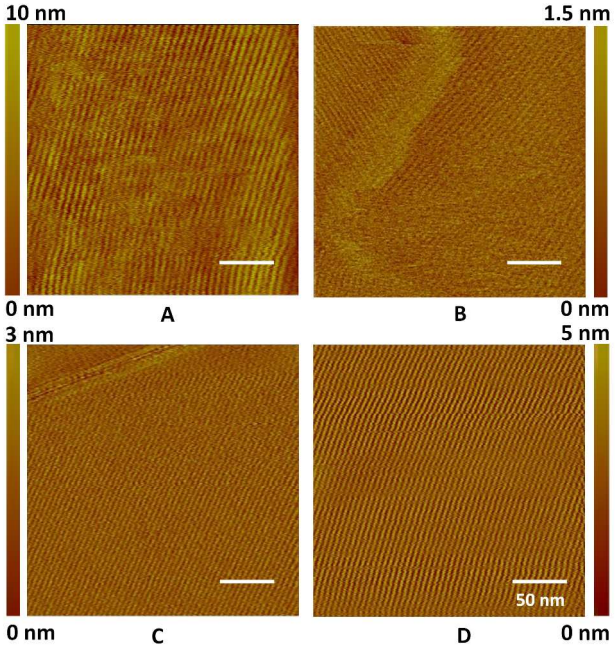

Figure 1. Vertical deflection images of adsorbed SDS micellar films at graphite surfaces from (A) 7.5 mM SDS, (B) 10 mM SDS, (C) 15 mM SDS, and (D) 15mM SDS in 20 mM NaCl.

Breakthrough Force of SDS Film with Added Salt. With our ability to create and image stable surfactant films established, we looked to characterize the strength of the films via breakthrough forces. As the tip of the AFM approaches the surface, it encounters two sets of forces: DLVO repulsion or attraction, and steric/hydration forces. The former occurs over a large distance and terminates on contact with the surface, while the latter occurs while the tip is in contact or very near contact with the film. For silicon nitride tips (surface charge density,

$\sigma \sim -0.02\ C/m^2$) approaching a fully charged SDS film ($\sigma \sim -0.2\ C/m^2$) the expected scale of the repulsive DLVO force is on the order of 100 pN.[18, 20] As the tip exerts greater force on the surface than this, the film begins to deform and the force on the tip increases until a breakthrough event occurs. A labeled example of a breakthrough curve can be found in Figure 2A. The surface structures observed for SDS are comprised of tubular/wormlike hemimicelles. A cross sectional representation of the surface geometries involved in tip-surface contact can also be found in Figure 2B. While previous works with SDS films have not focused on measuring the breakthrough force, there is a significant body of literature that uses AFM to study the mechanical properties of similarly structured lipid films in this fashion. [12, 18, 21]

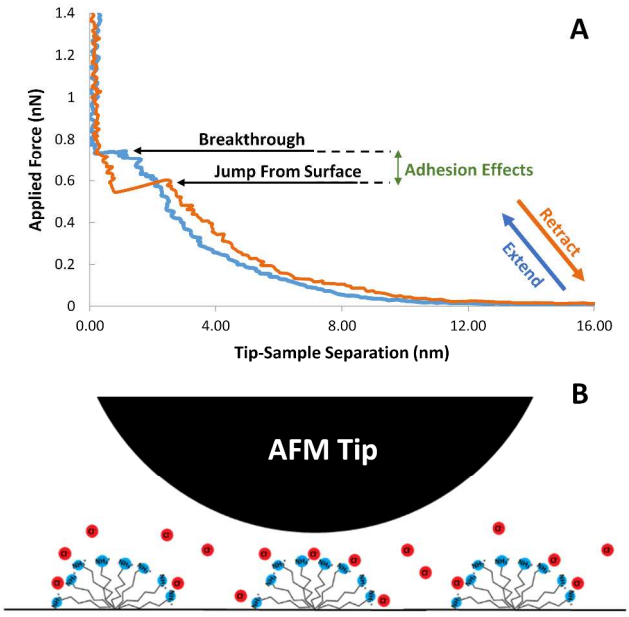

Figure 2. Shown are (A) an example of a force curve used to record a breakthrough event and (B) a proposed scheme of hemimicellar – tip geometry shown in cross-section. The force curve in (A) was taken for 10 mM DAH in the $MgCl_2$ dataset.

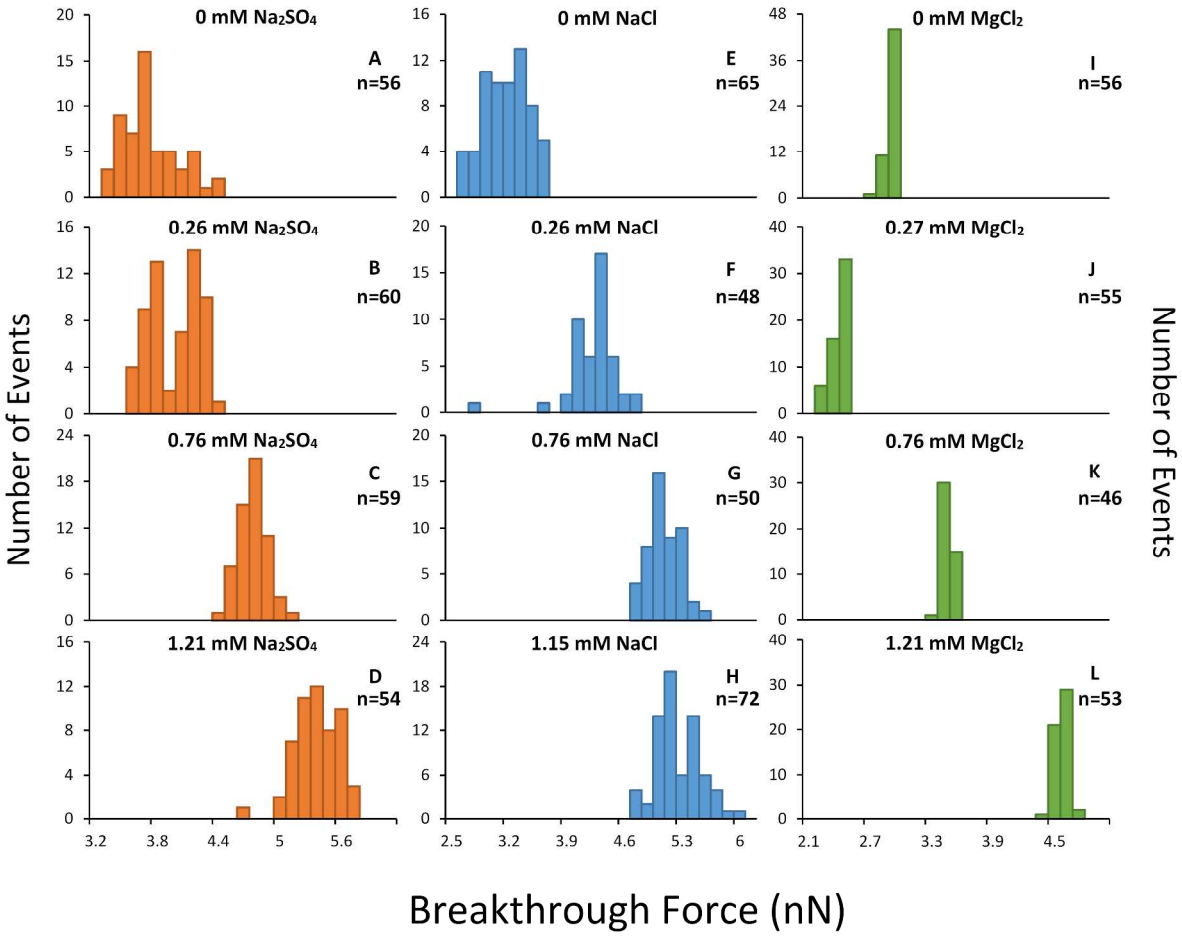

Figure 3. Breakthrough event distributions for 10 mM SDS micelles at a graphite surface with added Na_2SO_4 (A-D), NaCl (E-H), and $MgCl_2$ (I-L). The films probed are different between columns, as are the tips used. The sample sizes taken for each (n) are inset in the right of each graph.

We began our study of breakthrough forces by examining the effects of adding salts to SDS adsorbed onto graphite. Since breakthrough events are probabilistic in nature, it is not useful to record the force of a single event. Rather, a distribution of event forces must be assembled before any conclusions can be drawn. Shown in Figure 3 are histograms for breakthrough events at varying salt concentrations in 10 mM SDS solution. In lipid films, the range of breakthrough forces is much larger than what is observed here, with the maximum of observed forces often

being double that of the average.[18] It appears that for SDS films, however, the range of observable forces is much smaller, with the maximum observed force often being only 20% greater than the median. The differences in the range of observed forces may have to do with the structural difference between hemicylindrical and bilayer films. Much of the variation in breakthrough events in flat lipid layers comes from curvature fluctuations at the surface. These fluctuations are exacerbated by the wide planar geometry of most lipid films, where they can propagate far from the initial point of disturbance. The more contained nature of the hemicylindrical rows might hinder the propagation of such thermal disturbance, which would result in less noisy distributions of breakthrough events.

Gaussian fits were performed for each histogram in Figure 3 to find the center, which is typically taken to be the breakthrough force for the film. However, it was found for each curve that the average breakthrough force was always within 5% of the Gaussian center, and that the center of the fit varied within several percent depending on the choice of bin size. Since bin size is arbitrary, it was decided to use the average breakthrough force as the center, rather than the fitted Gaussian peak. For SDS, the average breakthrough force for a 10 mM film without any added salt was found to be 3 ± 0.3 nN (averaged over 5 tips and films), but observed average values ranged from 2 nN to 3.6 nN depending on the area probed and the tip used. The breakthrough depth was found to be 1.4 ± 0.3 nm over the same sample size. When the same tip and film were used, it was found that the average breakthrough force was generally consistent within micellar grains, but could change by up to 30% across grain boundaries. Since the variations in film strength due to salt addition were often less than this, efforts were made to minimize disturbances in breakthrough force measurements by both fixing the area probed and using the same tip during the course of a measurement. As such, each data point taken for a

given salt species is taken using the same tip, measuring the same area of surface, and using the same ramp rate. Measurements taken using forces far exceeding the breakthrough, with very high ramp rates, or applied continuously over long periods of time (>40 minutes) were observed to deteriorate the film strength. We avoided such conditions in our experiments, and no significant degradation was observed.

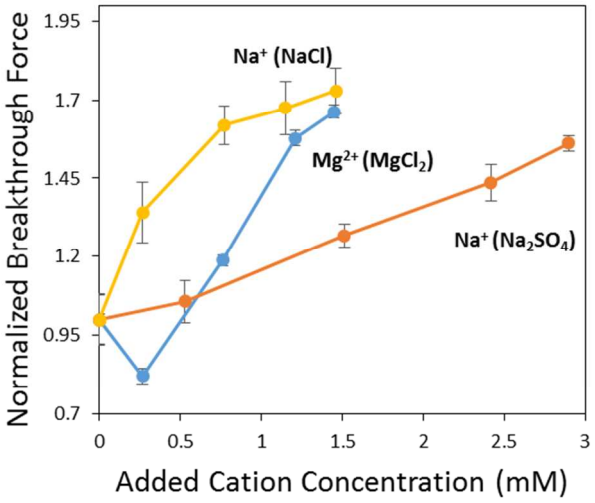

Figure 4. Normalized breakthrough forces for 10 mM SDS micelles at a graphite surface with various counterions and coions. Error bars shown represent the width of the normalized sample standard deviation.

Shown in Figure 4 are the effects of adding $MgCl_2$, NaCl, or Na_2SO_4 on the breakthrough force of a 10 mM SDS film. It should be noted that each point represents an average taken from the histograms in Figure 3, and that error bars represent the width of the standard deviation rather than any confidence interval. Results in Figure 4 have also been normalized by the initial breakthrough force, so as to eliminate the effect of the surface on initial film strength. We see that even at small salt concentrations a significant effect can be observed on the relative strength of the film, with the normalized breakthrough force increasing by roughly 70% for both $MgCl_2$

and NaCl and 55% for Na_2SO_4 at concentrations of only 1.5 mM. Our initial hypothesis was that the counterion would play a dominant role in any strengthening effects at the surface, which is why the horizontal axis of Figure 4 is measured by cation concentration rather than total ion concentration. The reasoning behind this was that, in lipid systems, the addition of counterions, and salts in general, causes the formation of salt bonds.[22] These bonds form between the lipid head groups, and similar bonds have been shown to cause greater packing density in surfactants such as SDS.[23] It has been shown for zwitterionic lipids, for example, that addition of salt can lead to very large increases in the breakthrough force.[18] Because this was our expected strengthening mechanism for the film, we also anticipated the strength of films with added magnesium to be much higher than films with added sodium. This would be due to the much greater binding affinity of divalent ions when compared to monovalent ions.[24] However, there are significant differences between the expected outcome and our observed results. Notably, the strength of the film is not independent of the coion concentration. Even though Na_2SO_4 and NaCl share the same cation, the effect of cation concentration on the surface strength is very different. We also observe an initial drop in the strength of the surface film when magnesium is present. This drop does not appear for either of the sodium salts, and the final strength of the film at 1.5 mM Mg^{2+} is less than that of NaCl at the same concentration. In addition to this, the observed effects of salt bridging in lipid layers are much less sensitive to concentration, with an expected increase in film strength of only 10% at 1 mM.[18] The images taken of SDS films as salts were added showed no apparent relationship between periodicity and breakthrough force. Images and micellar spacing of these films in the presence of salts can be found in Supporting Information. It is clear, then, that the effects of salt addition are not easily characterized in the same way as a lipid film.

Binding Model. To better understand the effects of salt addition on the surface conditions of these films we developed a simplified model of our surface. The SDS film is considered a flat surface, with a surface charge density taken from literature of $\sigma_0 = -0.262$ C/m^2 when completely dissociated.[25] From here, we use modified versions of the Grahame equation (see Supporting Information) to calculate the surface potential ψ_0. The equations for each ion type are shown below.

(1a) $$\sigma^2 = 2\varepsilon\varepsilon_0 kT\left([Mg^{2+}]_\infty\left(e^{-2e\psi_0/kT} + 2e^{e\psi_0/kT} - 3\right) + [Na^+]_\infty\left(e^{-e\psi_0/kT} - 1\right) + [DS^-]_\infty\left(e^{e\psi_0/kT} - 1\right)\right)$$

$MgCl_2$

(1b) $$\sigma^2 = 2\varepsilon\varepsilon_0 kT\left([Cl^-]_\infty\left(e^{e\psi_0/kT} - 1\right) + [Na^+]_\infty\left(e^{-e\psi_0/kT} - 1\right) + [DS^-]_\infty\left(e^{e\psi_0/kT} - 1\right)\right)$$

NaCl

(1c) $$\sigma^2 = 2\varepsilon\varepsilon_0 kT\left(\left[SO_4{}^{2-}\right]_\infty\left(e^{2e\psi_0/kT} - 1\right) + [Na^+]_\infty\left(e^{-e\psi_0/kT} - 1\right) + [DS^-]_\infty\left(e^{e\psi_0/kT} - 1\right)\right)$$

Na_2SO_4

Where the concentrations denote the bulk values, e is the unit of elementary charge, ε is the relative permittivity of water, ε_0 is the permittivity of free space, and k is the Boltzmann constant. In this case, the dodecylsulfate concentration $[DS^-]_\infty$ is taken to be the same as the CMC of 7.8 mM for SDS, as it is the free DS^- ion concentration in solution. If no additional ions are added to the solution and no binding is occurring, a Boltzmann distribution indicates that the surface concentration of Na^+ ions is roughly 11.7 M. This is far above the solubility of NaCl or SDS, and as such it is clear we must factor in the effects of binding on the surface charge density if we are to make use of this model. From literature, we can find that the fractional dissociation

of SDS when in micellar form is only about 0.27, meaning that 73% of the surface is neutralized on average.[26] If we model binding of ions to the surface as a Langmuir isotherm, our degree of surface coverage, θ_i, by a given ion is given by the relation,

$$\theta_i = \frac{K_i[C_i]_0{}^{n_i}}{1+\sum_j K_j[C_j]_0{}^{n_j}} . \quad (2)$$

Where K_i is an equilibrium constant given by the equation $K_i = \frac{[C_i S]}{[C_i]_0{}^{n_i}[S]}$ with [S] being the number of surface sites, n_i being a factor relating to adsorption stoichiometry, and $[C_i]_0$ being the concentration of ions at the surface. From the information about dissociation at the surface, and assuming $n_{Na^+} = 1$, we can calculate the surface potential when $\sigma = 0.27\sigma_0$ and the subsequent sodium ion concentration at the surface of 1.5 M (see Supporting Information). This method of calculation gives us a surface potential of -128 mV, which is in good agreement with the literature values that place it between -140 mV and -120 mV.[25] Using equation (2) then, our equilibrium constant for sodium is roughly 1.8 M^{-1}.

Now we examine how the system changes when ions are added to the solution. We begin with magnesium, as this is the system where we most expect surface binding to matter. Literature information of the binding of magnesium to dodecylsulfate ions is sparse, but data exists for calcium and sodium. It was found that the surface fraction bound by calcium for 10 mM SDS was roughly 0.65 when the calcium concentration was 0.3 mM.[24] It has also been shown from conductivity measurements that the surface charge density of magnesium dodecylsulfate micelles is roughly 4/3 that of calcium dodecylsulfate micelles.[27] From these pieces of information, and assuming $n_{Mg^{2+}} = \frac{1}{2}$ due to its double charge, we can estimate the equilibrium constant for magnesium binding at the micellar surface as $K_{Mg} \sim 2.1\ M^{-\frac{1}{2}}$ (see Supporting Information). We

are assuming in our model that magnesium binds to a single site first before attaching to a second adjacent site, though this is only a simplification.

With the equilibrium constants, we can now look at the degree of binding at the surface with respect to $MgCl_2$ concentration. Using equations (1a) and (2) we find that at magnesium ion concentrations of 0.25 mM the fraction of our surface that has been neutralized by magnesium is nearly 0.45 (see Supporting Information). Further increases in magnesium concentration cause only small changes in the overall surface binding, with the final neutralized fraction resting at 0.75 at a bulk magnesium ion concentration of 3 mM. Looking at Figure 4, we see that the drop in film strength when magnesium is added occurs only at very low concentrations. That the binding of magnesium ion and the dip in film strength occur simultaneously implies a connection, though this does not explain the cause of the film's subsequent strengthening at higher concentrations.

When we do these calculations with sodium sulfate and sodium chloride at 3 mM compared to 0 mM, we find that the degree of binding at the surface changes by a fraction of only $4x10^{-4}$, and the surface counterion concentration changes by only 0.2%. This reinforces the idea that bridging, which is the primary strengthening mechanism for lipid films when in the presence of counterions, is not the mechanism for strengthening here, as the change in surface conditions is too small to explain the large changes in film strength observed.

Free Energy. From our relatively simple model, we can see that the number of sodium counterions at the surface remains nearly unchanged at added concentrations of order 1 mM NaCl and Na_2SO_4. However, as these ions are added, a depletion profile (region of lower ionic concentration than bulk) of coions forms near the surface, which should result in a change in the surface's free energy. In previous works with lipid films, it has been shown that the breakthrough

of the tip to the surface below is a process dictated by a rate constant k_0 with an Arrhenius relationship $k_0 = {k_0}' e^{-\Delta G_0/kT}$ where ${k_0}'$is the frequency of breakthrough attempts, and ΔG_0 is the activation energy required to create an activation volume V and begin the process of film collapse. [13, 21] Franz et al. related the rate constant to the breakthrough force for a monolayer film with the equation,

$$F = \frac{A}{\alpha V} kT ln\left(\frac{K\nu}{kT}\frac{\alpha V}{A}\frac{1}{k_0}\right). \quad (3)$$

Where A is the contact area, α is a constant that relates to the shape of the free energy curve during and after activation, V is the activation volume, K is the spring constant of the cantilever, and ν is the load rate when measuring the breakthrough force.[16, 28] Substituting our relationship for k_0 into equation (3) we arrive at

$$F = \frac{A}{\alpha V} kT \left[ln\left(\frac{K\nu}{kT}\frac{\alpha V}{A}\frac{1}{{k_0}'}\right) + {\Delta G_0}/{kT} \right]. \quad (4)$$

If we acknowledge that the free energy of activation is effectively a free energy of dispersal, as it involves the creation of a void where a micelle existed, then any change in the free energy of activation caused by the addition of ions to solution should be matched by change in the free energy of micellization. That means that $\frac{\partial(\Delta G_0)}{\partial C_i} = -\frac{\partial(\Delta G_{micellization})}{\partial C_i}$, so if we can relate the free energy of micellization to the concentration of ions in solution then we can formulate a relation between the breakthrough force and the concentration of ions. This relationship is well known for spherical micelles to be

$$\Delta G_{micellization} = (2-\beta) kT ln\left(\frac{C_{CMC}}{1M}\right). \quad (5)$$

Where β is the degree of surface ion dissociation.[29-30] Assuming that only the free energy changes with the CMC (our binding model suggests that β shows little variation when salts are added) and normalizing by the initial breakthrough force at $C_i = 0$ we arrive at the relation

$$\hat{F} = -\left(\frac{kTA}{F_0 \alpha V}\right)(2-\beta)\ln\left(\frac{C_{CMC}}{C^0_{CMC}}\right) + 1. \quad (6)$$

Where $\hat{F}$ is the normalized breakthrough force, F_0 is the initial breakthrough force, and C^0_{CMC} is the CMC of the pure surfactant. A more detailed derivation can be found in Supporting Information. This means that if we know the CMC of a given surfactant and salt mixture, we should be able to relate it to the expected change in breakthrough force. We must note that equation (3) was derived for a flat monolayer, and that our tip-surface geometry (See Figure 2B) is significantly different. The most important difference is that our film thickness depends on tip position, and whether the tip is directly over a micelle or not. For large tip diameters, we expect our results to approach those of a flat monolayer. Our tip diameter is roughly two micellar spacings wide, however, which may not be wide enough to ignore position dependent effects. Since we observe breakthrough events in nearly all force curves, there is reason to believe our tip is large enough for equation (3) to apply. We continue analysis understanding that equation (6) is only an approximation, and that some error is present due to our surface geometry.

CMC Measurements and Breakthrough Force with Added Salt. In order to measure how the CMC of these solutions changes with added ion concentrations, we turned to fluorescence anisotropy measurements. We used 1,6-diphenyl-1,3,5-hexatriene (DPH), a fluorescent probe, to measure the changes in sample polarization with increasing SDS concentration. Once micelles form in solution, the DPH rapidly imbeds itself within them due to its strong hydrophobicity. This changes the procession time of these molecules and the resultant effect on polarization can

be measured via fluorescence polarization spectra measurements. Fluorescence anisotropy is often used to study phase changes in lipids and surfactants, and its usefulness in determining CMC values is well documented.[31-32] Shown in Figure 5A are the measured CMC values of SDS for each added salt.

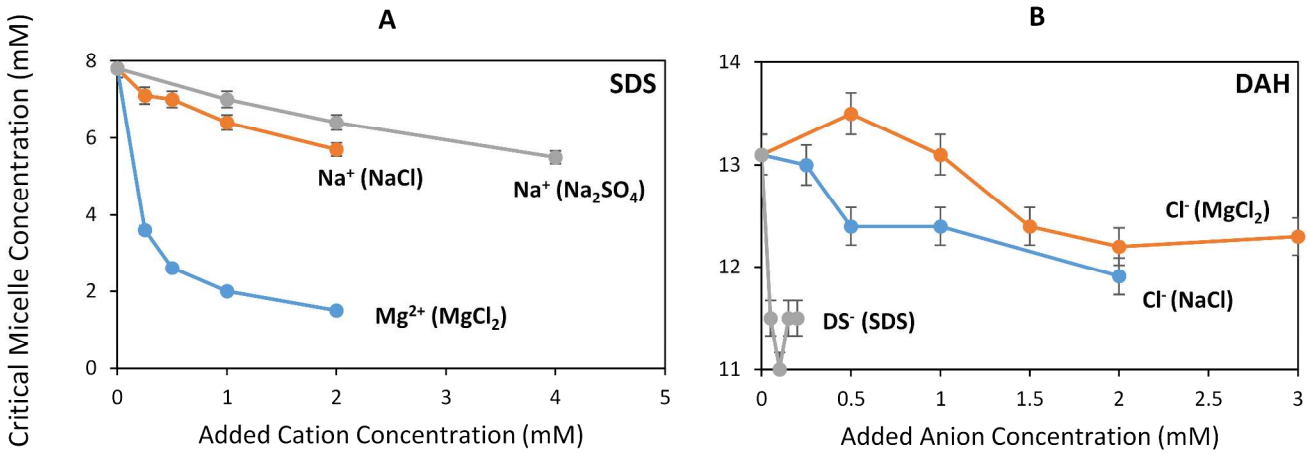

Figure 5. Shown are measured CMC values for SDS (A) and DAH (B) in the presence of added counterions. Error bars represent a fixed percentage error.

In order to interpolate our CMC data for SDS, these values were then fit empirically using an equation of the form $C_{CMC} = C_{CMC}^{0} e^{-DC_i^E}$ where D and E are fitting constants. Data from the binding model and Figure 5 was then combined with equation (6) to create a model curve (see Supporting Information), shown in Figure 6A for NaCl and Na_2SO_4, fitted to the relation $\hat{F} = -(X)(2-\beta)\ln\left(\frac{C_{CMC}}{C_{CMC}^{0}}\right) + 1$ where X is a fitted constant that includes the activation volume, V. A summary of the major variables involved in fitting can be found in the Supporting Information section. The resulting model shows good agreement with the gathered data for NaCl and Na_2SO_4. The results for $MgCl_2$ are in poor agreement (data not shown) in the range where ion binding occurs - one possible explanation for this lies with the dependence of V on the ratio

of bound Na^+ to Mg^{2+} ions. From the modelled curves, we can obtain activation volumes if we are willing to make assumptions about the contact radius and the value of α. Assuming a tip radius of 6 nm with a hemispherical contact area, as well as an α value of 0.5, [33] which corresponds to a system where the free energy barrier is symmetrical, we arrive at an activation volume of roughly 0.4 nm^3 for both NaCl and Na_2SO_4 solutions and 0.8 nm^3 for $MgCl_2$ solutions using a still unacceptable fit shown in Figure 6B (orange curve), where the added constant can vary from a value of 1. These values are nearly equal to displacing 1-2 molecules of SDS at the surface, which may be plausible given the tight size of the micellar structures. However, these are order of magnitude estimates due to the ambiguity of the interaction geometry and tip size.

The unacceptable fit for the normalized breakthrough force of SDS micelles in $MgCl_2$ solutions may indicate that equation (6) should be modified for cases where the activation volume is not independent of added salt concentration. While activation volume generally increases with tip size and radius of curvature, it can also shift if the surface mobility changes within the film. If we allow activation volume to change with salt concentration, we arrive at the equation

$$\hat{F} = \left(\frac{kTA}{F_0 \alpha V_0}\right) \ln\left(\left(\frac{K\nu V\alpha}{kTAk_0{}'}\right)^{\frac{V_0}{V}-1} \left(\frac{V}{V_0}\right) \frac{C_{CMC}^{0\,(2-\beta_0)}}{C_{CMC}^{\frac{V_0}{V}(2-\beta)}}\right) + 1. \quad (7)$$

Where V_0 and β_0 are the initial activation volume and dissociation fraction respectively. A more detailed derivation of this can be found in Supporting Information. Using equation (7) along with our binding model from equations (1a) and (2) to estimate values for β, and an average of obtained V_0 values from the sodium chloride and sodium sulfate trials of 0.37 nm^3, we can fit our results to equation (8).

(8) $$\hat{F} = \left(\frac{Z}{V_0}\right) \ln\left((YV)^{\frac{V_0}{V}-1} \left(\frac{V}{V_0}\right) \frac{{C_{CMC}^0}^{(2-\beta_0)}}{{C_{CMC}}^{\frac{V_0}{V}(2-\beta)}} \right) + 1$$

Where Z is taken to be 0.325 x 10^{-28} m^3 (from previously assumed values) and Y is a constant. The value of Y is taken to be 2.07x10^{22} m^{-3}, and can be calculated assuming a K of 0.05 N m^{-1}, a ν of 50 nm s^{-1}, a tip radius of 6 nm with hemispherical contact area, a k_0' equal to the resonant frequency of the tip in water (65 kHz), and an α of 0.5. A table containing the source of each value used in fitting can be found in the Supporting Information section. It is important to note that we are fitting activation volumes to our data, as we have no information that relates the degree of surface binding to the change in activation volume. This means our model should always match reasonably with experimental results, and that we should be more interested in the activation volumes it produces than the quality of the fit. Results of the new model are compared with the initial model in Figure 6B, and are shown alongside the fitted activation volumes in Figure 6C.

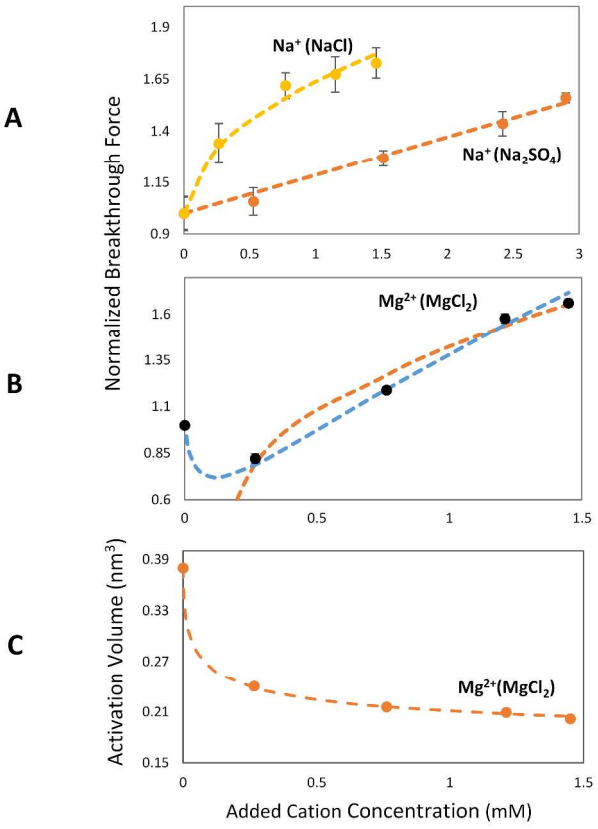

Figure 6. Shown are the results of fitted models for normalized breakthrough forces of 10 mM SDS micelles using measured CMC values in (A) NaCl and Na_2SO_4 and (B) $MgCl_2$. Both model curves in (A) use equation (6). In (B), the orange curve represents a fit using fixed activation volume and variable added constant in equation (6) and the blue curve represents a fit using variable activation volume and equation (7). The fitted activation volumes (points) for (B) are plotted against added cation concentration in (C). The dotted line in (C) represents a fitted function that uses our binding model in equations (1a) and (2) as well as equation (9).

The model using variable activation volume in Figure 6B (blue curve) is a much better fit than our initial attempts, accurately depicting the observed dip in film strength seen at low magnesium concentrations. Of particular interest, however, are the activation volumes that are required to achieve this fit. We see from Figure 6C that, aside from an initial decrease, the set of

activation volumes that satisfies our observed results is nearly constant. The activation volume V near 1.5 mM approaches a value of 0.21 nm^3, and the overall shape of the curve indicates that the activation volume changed largely at low concentrations and remained nearly constant at higher concentrations. The dotted line in Figure 6C represents fitted results of our binding model described by equations (1a) and (2), where we assumed that the overall activation volume was determined by the linear relationship

$$V = V_{Mg^{2+}} f_{Mg^{2+}} + V_{Na^{+}}(1 - f_{Mg^{2+}}). \quad (9)$$

Where $f_{Mg^{2+}}$ is the fraction of bound sites occupied by magnesium, $V_{Na^{+}}$ is the activation volume when only sodium is present, and $V_{Mg^{2+}}$ is the activation volume when only magnesium is present. Our model fit obtained a $V_{Mg^{2+}}$ of 0.16 nm^3, which is significantly smaller than that of $V_{Na^{+}}$ at 0.38 nm^3. That $V_{Mg^{2+}}$ is significantly less than $V_{Na^{+}}$ implies that the surface mobility of magnesium bound surfactant molecules in the micelles is much higher than the surface mobility of sodium bound surfactant molecules, as the activation volume is also a measure of the self-diffusion of surfactant molecules within the film.[33]

Breakthrough Force of DAH Film with Added Salt. To explore the effects of ion addition on cationic surfactants, we also imaged dodecylamine hydrochloride (DAH) films on the graphite substrate. This ion was chosen because it has been previously theorized and shown to form the same hemicylindrical micelles at hydrophobic surfaces as observed in SDS.[34-35] We were able to observe DAH hemimicelles at the surface at concentrations as low as 7.5 mM (see Supporting Information). These micelles were larger than those seen in SDS, with intermicellar spacing of roughly 7.8$\pm$0.1 nm at a concentration of 10 mM. It should be noted that this is below the 13.1 mM critical micelle concentration (CMC) of DAH in solution. At concentrations well above the

CMC of DAH, the intermicellar spacing was found to stabilize around 4.1±0.1 nm, which is on par with that of SDS.

The breakthrough force for a 10 mM DAH film in the absence of salts was found to be 1.1 ±0.1 nN using a sample of 4 films and tips (see Supporting Information for breakthrough force event distributions). The breakthrough depth calculated using the same data sets was found to be 1.9 ±0.2 nm. Breakthrough force measurements were performed with added salts to explore the effect of the surface charge on mechanical strength as it relates to ion addition. Figure 7A displays our measurements for the relative breakthrough forces of DAH and the modeled results from Equation (6), where the modeled data used CMC measurements given in Figure 5B. Similar to our SDS results, we observe a decrease in the CMC and a resultant increase in the breakthrough force with added NaCl, with the overall strength of the DAH film increasing by a factor of 1.5. We also observe an initial dip in the breakthrough force with the addition of $MgCl_2$ similar to what was seen in the SDS system, though the reason for this appears to be different. In the case of DAH, we can see from the data in Figure 5B that the CMC of DAH was found to increase when small amounts of $MgCl_2$ were added, implying that the change in surface strength is due to a surface free energy change rather than a change in activation volume. AFM images of the surface during the addition of $MgCl_2$ showed a monotonic decrease in micellar spacing, which does not explain the observed dip in film strength (see Supporting Information).When fitting our DAH data to the activation energy model for NaCl using the CMC values obtained in Figure 5B, we obtain an activation volume of 0.3 nm^3, which is close to the literature values of 0.35 nm^3 for the volume of a DAH molecule.[36] Our fitted data for DAH when $MgCl_2$ was added used a constant activation volume of 0.86 nm^3, which is still within an order of magnitude of the result for NaCl. This is consistent with our SDS results, implying that the activation volume

required to initiate breakthrough is on the order of the volume of one molecule in these structures.

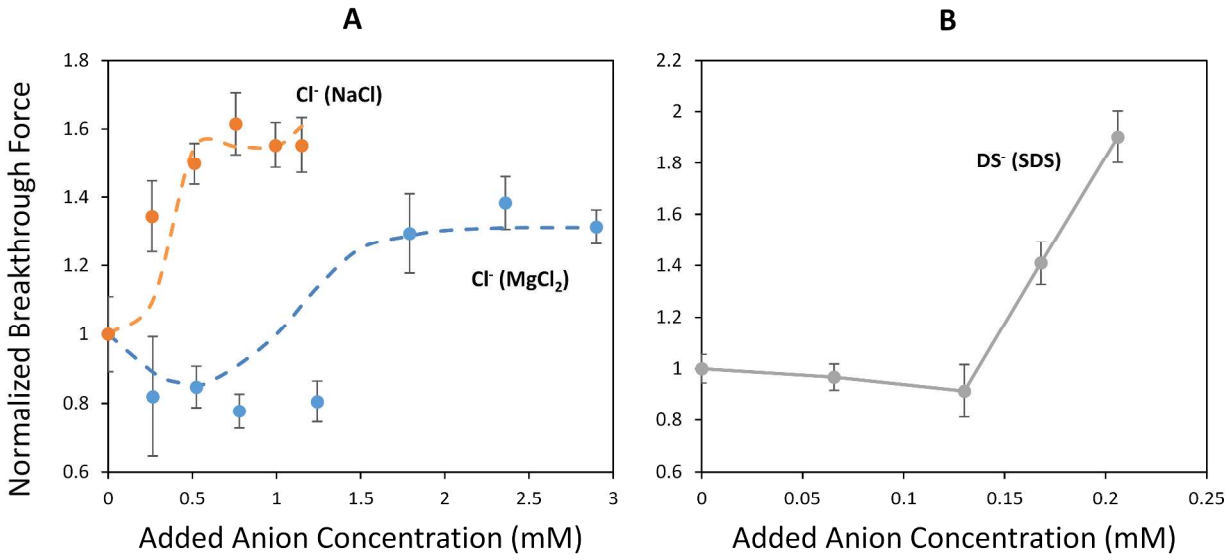

Figure 7. Normalized breakthrough forces for 10 mM DAH micelles at a graphite surface with various counterions and coions. Dotted lines represent fitted models using measured CMC values and equation (6) (A). The solid line (B) seen for the DAH with added SDS is a visual aid only. Error bars shown represent the width of the normalized standard deviation.

Breakthrough Force with Addition of Counterion Surfactant. Shown in Figure 7B is the result on film strength of adding SDS to a 10 mM DAH film. The breakthrough force increases twofold after addition of only 0.2 mM of SDS. It should be noted that concentrations of SDS above this point resulted in high amounts of turbidity, which made imaging of the surface and resolution of breakthrough forces impossible. Similar experiments were attempted for 10 mM SDS films with added DAH, but in these trials a second film readily formed on the tip and interfered with results. While the effect of counterion surfactant addition is clearly strong, it may not share the same strengthening mechanism as observed when salts are added. Attempts to use

equation (6) to model the film strength failed, as the CMC data does not reflect the observed trends in the normalized breakthrough force. There is also little data on binding constants between SDS and DAH, making modeling using equation (7) difficult. In this case, however, AFM images may reveal the mechanism of strengthening. Shown in Figure 8 are images taken of the DAH film as SDS is added. Dark and bright spots in these images represent irregularities at the surface, and a graphite step is observable on the left side of Figure 8C. At 0.13 mM SDS added, the surface film shows significant changes and irregularities in its packing. Once the concentration of SDS reaches 0.2 mM, the film has become almost completely flat. This implies that the mechanism for strengthening in the case of added counterionic surfactant may be a phase change rather than a strict surface energy change.

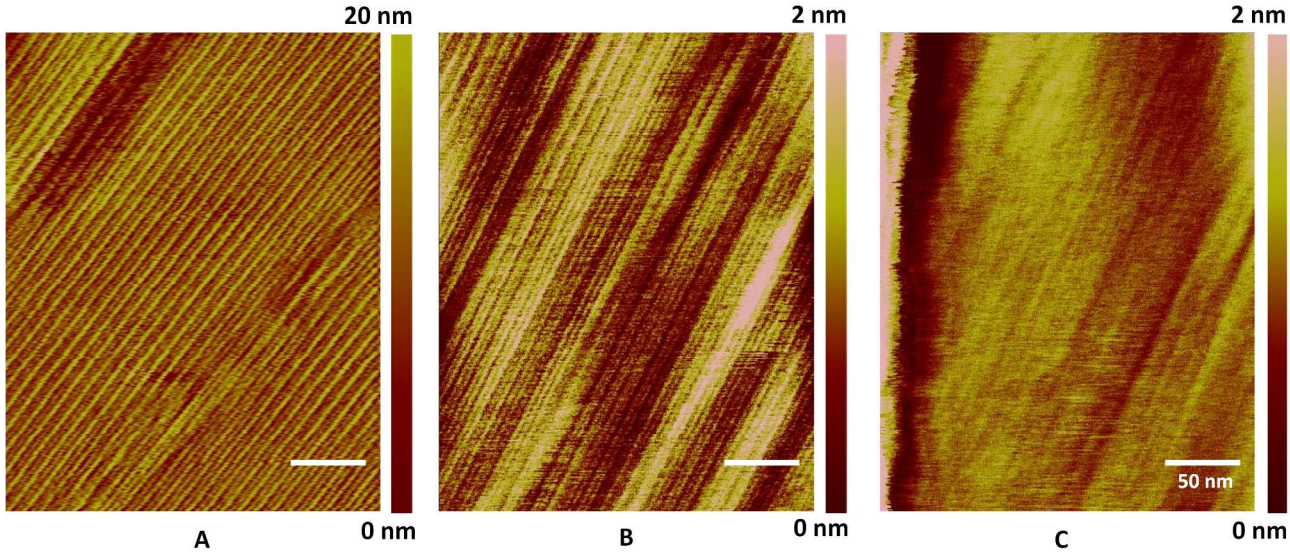

Figure 8. Vertical deflection images showing the transitions of a 10 mM DAH film as SDS is added. Shown are SDS concentrations of (A) 0 mM, (B) 0.130 mM, and (C) 0.206 mM.

Breakthrough Force with Change in pH. We examined the effect of pH change on film strength. In order to prevent the skewing of results due to counterion binding, only HCl was

added to SDS and only NaOH was added to DAH. We could not measure meaningful changes in CMC values with pH via fluorescence anisotropy due to the difficulty in maintaining exactly the same pH over a broad range of surfactant concentrations. Therefore quantitative application of equations (6) or (7) was not possible.

For an SDS film, normalized breakthrough force increased to 1.1 at ~pH 3.5 and then decreased to 0.9 at ~pH 2.8 (Figure 9A). Using a pK_a value for SDS of 1.8, we can determine from our ion binding model at what concentrations there exists significant surface neutralization.[37] In the case of SDS, the pK_a gives an equilibrium coefficient of $K_{H_3O^+} = 10^{1.8} = 63\ M^{-1}$. Using this value, we calculate that when the bulk solution is at a pH of 3, the surface is actually at a pH of 1.2, and is already 65% neutralized by hydronium ions. At bulk pH values below 2.78, we observed precipitation in the solution; our model suggests that the pH at the surface at this point is roughly 1.1, with a surface neutralization fraction of 0.78 from hydronium ions alone and 0.84 overall, i.e. $\beta = 0.16$ where $\beta_0 = 0.27$. In addition to this, literature suggests that decreasing the pH of an SDS solution should result in a decrease in the CMC.[38] According to equation (7), these factors should result in an overall increase in the normalized breakthrough force if the activation volume remains constant. However, if the activation volume of SDS micelles bound by hydronium ions is smaller than that of SDS micelles bound by sodium ions, similar to the case for added magnesium ions, then the decrease in overall activation volume could overcome the CMC effect and lower the breakthrough force. As such, we speculate that the initial rise in film strength is a result of decreasing CMC and β, while the subsequent drop at lower pH values is caused by a decrease in the activation volume.

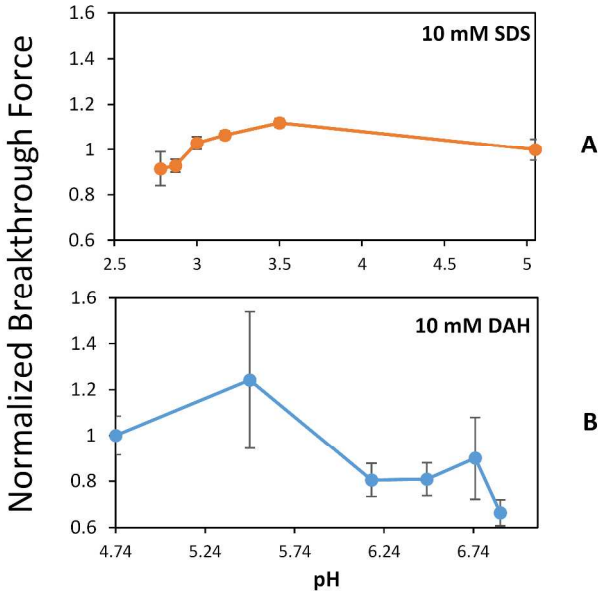

Figure 9. Normalized breakthrough forces at various pH values for 10 mM SDS (A) and 10 mM DAH (B) films at a graphite surface. Error bars represent the normalized standard deviation.

The trend in normalized breakthrough force of 10 mM DAH when pH is increased (Figure 9B) is similar to that of 10 mM SDS when pH is decreased (Figure 9A), although the magnitudes of the increase followed by decrease are larger. Unlike the SDS system, the dissociated surface fraction of DAH does not change significantly with pH, with the final and initial value being ~ $\beta = 0.18$ (see Supporting Information). It has been shown that the CMC of DAH decreases with increasing pH[39] and equation (7) predicts an increase in average normalized breakthrough force with decreasing CMC as observed at pH 5.5. As the pH continues to increase, the number of deprotonated ammonium groups must also increase to maintain equilibrium with the decreasing number of hydronium ions. Realizing that we go from an initial surface pH of 5.9 to a final pH of 8.1, we can conclude that the ratio of deprotonated ammonium groups to protonated groups must increase by a factor of over 100. We invoke once again speculation that the overall activation

volume was decreased by this change in ionic state of the micelles, resulting in a decreased normalized breakthrough force.

CONCLUSIONS

We have shown that we can measure breakthrough forces for hemimicellar surfactant films composed of SDS or DAH, and we can relate the change in breakthrough force associated with the addition of salts to the change in critical micelle concentration for the primary surfactant. The mechanism for this strengthening is distinct from what has been previously seen in lipid layers, as it is far more sensitive to ionic concentration and surface free energy than previous work with lipids would suggest. In the case where magnesium ions bind to the surface, we observed an unexpected initial drop in film strength. By adjusting our model to allow for changing activation volume for SDS micelles, we have shown that our results can be explained by a decrease of our activation volume from a value of 0.37 nm^3 to 0.21 nm^3. Addition of SDS to a primarily DAH solution was shown to cause a phase change at the surface from rows of hemicylindrical micelles to a flat planar structure. This resulted in an abrupt increase in the measured strength of the film. Work with both SDS and DAH suggested that changing the pH of the solution slightly decreased film strength and neutralized the surface, which occurred more readily due to the difference between surface and bulk pH. Our results make it clear that prediction of surface strength requires a better model for the binding of ions at the surface, as well as a means of determining changes in activation volume due to such binding. Further work should be done to study how activation volumes are affected by ion binding and ion sizes, and to determine how phase changes will affect film strength. Nevertheless, our model may serve as a basis for predicting how the mechanics of surfactant films at hydrophobic interfaces change in the presence of added ions and surfactants.

AUTHOR INFORMATION

Corresponding Author

*E-mail: mllongo@ucdavis.edu. Tel: 530-848-9340.

ACKNOWLEDGMENTS

Acknowledgment is made to the Donors of the American Chemical Society Petroleum Research Fund for support of this research under grant number 54813-ND5.

ASSOCIATED CONTENT

Supporting Information. Detailed derivations, images, and datasets can be found in the Supporting Information section. This is available free of charge on the ACS Publications website at http://pubs.acs.org.

REFERENCES

1. Manne, S.; Cleveland, J. P.; Gaub, H. E.; Stucky, G. D.; Hansma, P. K., Direct Visualization of Surfactant Hemimicelles by Force Microscopy of the Electrical Double Layer. *Langmuir* **1994,** *10* (12), 4409-4413.

2. Wanless, E. J.; Ducker, W. A., Organization of Sodium Dodecyl Sulfate at the Graphite−Solution Interface. *J. Phys. Chem.* **1996,** *100* (8), 3207-3214.

3. Zhang, S.; Teng, H. N., Rheology and microstructure studies of SDS/CTAB/H2O system. *Colloid J.* **2008,** *70* (1), 105-111.

4. Fielden, M. L.; Claesson, P. M.; Verrall, R. E., Investigating the Adsorption of the Gemini Surfactant "12−2−12" onto Mica Using Atomic Force Microscopy and Surface Force Apparatus Measurements. *Langmuir* **1999,** *15* (11), 3924-3934.

5. Fleming, B. D.; Wanless, E. J., Soft-contact Atomic Force Microscopy Imaging of Adsorbed Surfactant and Polymer Layers. *Microsc. Microanal.* **2000,** *6* (2), 104-112.

6. Paruchuri, V. K.; Nalaskowski, J.; Shah, D. O.; Miller, J. D., The effect of cosurfactants on sodium dodecyl sulfate micellar structures at a graphite surface. *Colloids Surf., A* **2006,** *272* (3), 157-163.

7. Wang, L.; Wang, E., Controlled Rearrangement of Adsorbed Undecanol Films on Mica Surfaces Induced by an Atomic Force Microscopy Tip. *Langmuir* **2004,** *20* (7), 2677-2682.

8. Fleming, B. D.; Wanless, E. J., Soft-contact atomic force microscopy imaging of adsorbed surfactant and polymer layers. *Microsc. Microanal.* **2000,** *6* (02), 104-112.

9. Ducker, W. A.; Wanless, E. J., Surface-Aggregate Shape Transformation. *Langmuir* **1996,** *12* (24), 5915-5920.

10. Wanless, E. J.; Davey, T. W.; Ducker, W. A., Surface Aggregate Phase Transition. *Langmuir* **1997,** *13* (16), 4223-4228.

11. Dimitriadis, E. K.; Horkay, F.; Maresca, J.; Kachar, B.; Chadwick, R. S., Determination of Elastic Moduli of Thin Layers of Soft Material Using the Atomic Force Microscope. *Biophys. J.* **2002,** *82* (5), 2798-2810.

12. Garcia-Manyes, S.; Sanz, F., Nanomechanics of lipid bilayers by force spectroscopy with AFM: A perspective. *Biochim. Biophys. Acta, Biomembr.* **2010,** *1798* (4), 741-749.

13. Butt, H. J.; Franz, V., Rupture of molecular thin films observed in atomic force microscopy. I. Theory. *Phys. Rev. E: Stat., Nonlinear, Soft Matter Phys.* **2002,** *66* (3 Pt 1), 031601.

14. Ngwa, W.; Chen, K.; Sahgal, A.; Stepanov, E. V.; Luo, W., Nanoscale mechanics of solid-supported multilayered lipid films by force measurement. *Thin Solid Films* **2008,** *516* (15), 5039-5045.

15. Schneider, J.; Dufrêne, Y. F.; Barger Jr, W. R.; Lee, G. U., Atomic Force Microscope Image Contrast Mechanisms on Supported Lipid Bilayers. *Biophys. J.* **2000,** *79* (2), 1107-1118.

16. Franz, V.; Loi, S.; Müller, H.; Bamberg, E.; Butt, H.-J., Tip penetration through lipid bilayers in atomic force microscopy. *Colloids Surf., B* **2002,** *23* (2–3), 191-200.

17. Loi, S.; Sun, G.; Franz, V.; Butt, H.-J., Rupture of molecular thin films observed in atomic force microscopy. II. Experiment. *Phys. Rev. E* **2002,** *66* (3), 031602.

18. Garcia-Manyes, S.; Oncins, G.; Sanz, F., Effect of Ion-Binding and Chemical Phospholipid Structure on the Nanomechanics of Lipid Bilayers Studied by Force Spectroscopy. *Biophys. J.* **2005,** *89* (3), 1812-1826.

19. Garcia-Manyes, S.; Redondo-Morata, L.; Oncins, G.; Sanz, F., Nanomechanics of Lipid Bilayers: Heads or Tails? *J. Am. Chem. Soc.* **2010,** *132* (37), 12874-12886.

20. Sonnefeld, J., Determination of surface charge density parameters of silicon nitride. *Colloids Surf., A* **1996,** *108* (1), 27-31.

21. Loi, S.; Sun, G.; Franz, V.; Butt, H. J., Rupture of molecular thin films observed in atomic force microscopy. II. Experiment. *Phys. Rev. E: Stat., Nonlinear, Soft Matter Phys.* **2002,** *66* (3 Pt 1), 031602.

22. Bockmann, R. A.; Hac, A.; Heimburg, T.; Grubmuller, H., Effect of sodium chloride on a lipid bilayer. *Biophys J* **2003,** *85* (3), 1647-55.

23. Pandey, S.; Bagwe, R. P.; Shah, D. O., Effect of counterions on surface and foaming properties of dodecyl sulfate. *J Colloid Interface Sci* **2003,** *267* (1), 160-6.

24. Maneedaeng, A.; Haller, K. J.; Grady, B. P.; Flood, A. E., Thermodynamic parameters and counterion binding to the micelle in binary anionic surfactant systems. *J. Colloid Interface Sci.* **2011,** *356* (2), 598-604.

25. Hartland, G. V.; Grieser, F.; White, L. R., Surface potential measurements in pentanol-sodium dodecyl sulphate micelles. *J. Chem. Soc., Faraday Trans. 1* **1987,** *83* (3), 591-613.

26. Sasaki, T.; Hattori, M.; Sasaki, J.; Nukina, K., Studies of Aqueous Sodium Dodecyl Sulfate Solutions by Activity Measurements. *Bull. Chem. Soc. Jpn.* **1975,** *48* (5), 1397-1403.

27. Goddard, E. D., The Influence of Calcium and Magnesium Ions on Dodecyl Sulfate and Other Surfactant Anions. In *Monolayers*, American Chemical Society: 1975; Vol. 144, pp 67-82.

28. El Zein, R.; Dallaporta, H.; Charrier, A. M., Supported Lipid Monolayer with Improved Nanomechanical Stability: Effect of Polymerization. *J. Phys. Chem. B* **2012,** *116* (24), 7190-7195.

29. Chang, N. J.; Kaler, E. W., The structure of sodium dodecyl sulfate micelles in solutions of water and deuterium oxide. *J. Phys. Chem.* **1985,** *89* (14), 2996-3000.

30. Mukerjee, P., The Thermodynamics of Micelle Formation in Association Colloids. *J. Phys. Chem.* **1962,** *66* (7), 1375-1376.

31. Zeno, W. F.; Hilt, S.; Aravagiri, K. K.; Risbud, S. H.; Voss, J. C.; Parikh, A. N.; Longo, M. L., Analysis of lipid phase behavior and protein conformational changes in nanolipoprotein particles upon entrapment in sol-gel-derived silica. *Langmuir* **2014,** *30* (32), 9780-8.

32. Zhang, X.; Jackson, J. K.; Burt, H. M., Determination of surfactant critical micelle concentration by a novel fluorescence depolarization technique. *J. Biochem. Biophys. Methods* **1996,** *31* (3-4), 145-50.

33. El zein, R. Solid supported lipid monolayer : From biophysical properties to sensor application. Ph.D. Dissertation, Biophysique Aix-Marseille 2013.

34. Wang, X.; Liu, J.; Du, H.; Miller, J. D., States of Adsorbed Dodecyl Amine and Water at a Silica Surface As Revealed by Vibrational Spectroscopy. *Langmuir* **2010,** *26* (5), 3407-3414.

35. Nishimura, S.; Scales, P. J.; Biggs, S.; Healy, T. W., An Electrokinetic Study of the Adsorption of Dodecyl Ammonium Amine Surfactants at the Muscovite Mica−Water Interface. *Langmuir* **2000,** *16* (2), 690-694.

36. Mihelj, T.; Tomašić, V., Amphiphilic Properties of Dodecylammonium Chloride/4-(1-Pentylheptyl) Benzene Sodium Sulfonate Aqueous Mixtures and Study of the Catanionic Complex. *J. Surfactants Deterg.* **2014,** *17* (2), 309-321.

37. Sodium Lauryl Sulfate (Powder). TensaChem: Online.

38. Rahman, A.; Brown, C. W., Effect of pH on the critical micelle concentration of sodium dodecyl sulphate. *J. Appl. Polym. Sci.* **1983,** *28* (4), 1331-1334.

39. Dai, Q.; Laskowski, J. S., The Krafft point of dodecylammonium chloride: pH effect. *Langmuir* **1991,** *7* (7), 1361-1364.

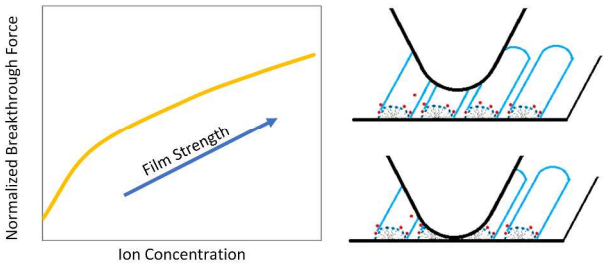
Normalized Breakthrough Force
Film Strength
Ion Concentration